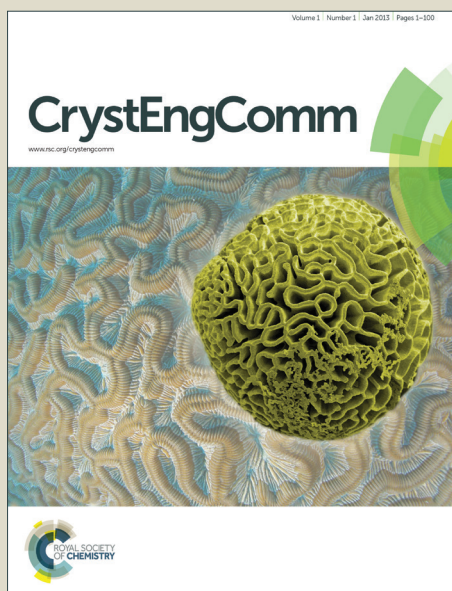


CrystEngComm

Accepted Manuscript



This is an *Accepted Manuscript*, which has been through the Royal Society of Chemistry peer review process and has been accepted for publication.

Accepted Manuscripts are published online shortly after acceptance, before technical editing, formatting and proof reading. Using this free service, authors can make their results available to the community, in citable form, before we publish the edited article. We will replace this *Accepted Manuscript* with the edited and formatted *Advance Article* as soon as it is available.

You can find more information about *Accepted Manuscripts* in the [Information for Authors](#).

Please note that technical editing may introduce minor changes to the text and/or graphics, which may alter content. The journal's standard [Terms & Conditions](#) and the [Ethical guidelines](#) still apply. In no event shall the Royal Society of Chemistry be held responsible for any errors or omissions in this *Accepted Manuscript* or any consequences arising from the use of any information it contains.

Effect of inductive effect on the formation of Cocrystals and Eutectics

Karothu Durga Prasad,^a Suryanarayan Cherukuvada,^a L. Devaraj Stephen^b and Tayur N. Guru Row^{a*}

^a Solid State and Structural Chemistry Unit, Indian Institute of Science, Bengaluru 560012, India

^b Department of Chemistry, SRM Valliammai Engineering College, Chennai 603203, India

* Email: ssctng@sscu.iisc.ernet.in

Abstract: There is a growing need to understand the factors that control the formation of different yet related multi-component adducts such as cocrystals, solid solutions and eutectics both from fundamental and application perspectives. Benzoic acid and its structural analogues, having gradation in inductive force strengths, are found to serve as excellent cofomers to comprehend the formation of above adducts with the antiprotozoal drug Ornidazole. Combination of the drug with para-amino and -hydroxybenzoic acids resulted in cocrystals in accordance to the induction strength complementarity between the participant hydrogen bond donor-acceptor groups. The lack of adequate inductive forces for combinations with benzoic acid and other cofomers was exploited to make eutectics of the drug. The isomorphous/isostructural relationship between para-amino and -hydroxybenzoic acid–drug cocrystals was utilized to make their solid solutions i.e. solid solutions of cocrystals. In all, we successfully steered and expanded the supramolecular solid form space of Ornidazole.

Introduction

Cocrystallization,¹ the art of making cocrystals for novel and desired applications, also encompasses the study of the formation of other multi-component organic solids such as solid solutions, eutectics etc.² However, as a phenomenon, it is less understood in terms of the factors that govern it and less studied as of reliably/specifically obtaining a desired cocrystallization product. In continuation to the recent efforts in improving the overall understanding of the cause and effect and thus success rate of cocrystallization,^{2a,b,3} we undertook the task of desirably making cocrystals, solid solutions of cocrystals, and eutectics in a series. The precedent for the formation of cocrystals is the occurrence of adequate heteromolecular interactions in the combination while for eutectics it is their absence.^{2a,b} Isomorphous and isostructural relationship between the components is well-known to result in solid solutions of their combination,⁴ but reports on solid solutions that are formed by cocrystals are sparse.⁵ In this study, we analyzed the inductive effect of hydrogen bonding functional groups on the formation of cocrystals and eutectics. Although inductive effect is more often referred in the context of covalent reactivity of functional groups,⁶ the generation of dipoles and consequent attractive/repulsive forces (electrophilicity/nucleophilicity) in the molecular niche is also relevant to their supramolecular reactivity i.e. non-covalent interactions in terms of supramolecular recognition and binding. Thus, higher the electronegativity difference and bond polarization in a functional group, greater will be its tendency to form electrostatic interactions with complementary functionalities.⁷ Altogether, the strength of hydrogen and halogen bonds, which are primarily electrostatic,⁷ depends both on the induction strength of donor and acceptor functional groups and their complementarity. Therefore, based on the relative differences in the electronic effects of hydrogen/halogen bonding groups, it should be possible to tune adduct formation given the variability in induction and electrostatics, and therefore interactions, for different combinations.

Ornidazole (abbreviated as ORL, Figure 1) is a third generation nitroimidazole solid drug with antiprotozoal and antibacterial effects⁸ and is listed in the Indian Pharmacopoeia.⁹ It is also marketed as a combination formulation with fluoroquinolone antibiotic Ofloxacin to treat bacterial infections.¹⁰ Further, it is indicated in the treatment of Crohn's disease¹¹ and poultry infections.¹² Several salts,¹³ a cocrystal¹⁴ and a hemihydrate¹⁵ of ornidazole were reported. ORL is high soluble¹⁶ and relatively stable^{8a,17} and hence solid-form screening with the objective of improving its physico-chemical properties is needless. However, to comprehend the cocrystallization phenomenon and thus obtain desired adducts,^{2b} ORL with its potent hydrogen bonding functionalities (nitro and imidazole groups) serves as an excellent model drug system. Benzoic acid and its structural analogues (Figure 1), having gradation in inductive force strengths of their functional groups, are selected as cofomers to form different adducts with ORL. Two cocrystals, two solid solutions of cocrystals, and three eutectics of the drug are obtained and the issues with respect to their formation are discussed. X-ray diffraction (XRD) and differential scanning calorimetry (DSC) are used to establish the integrity of the new adducts.

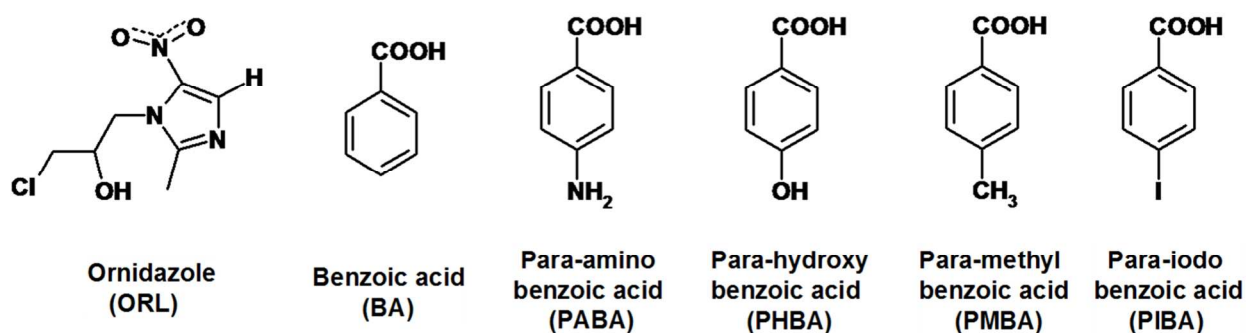


Figure 1 Molecular structures and acronyms of the compounds.

Results and Discussion

Cocrystallization experiments were carried out by solid-state grinding method^{2a,b,18} (detailed in Experimental Section). Ground products were analyzed by powder XRD and DSC to establish cocrystal/eutectic product based on the fact that the former shows distinct PXRD patterns and melting behavior and the latter shows only lowering in melting point as compared to parent materials.^{2a,b} Para-amino and -hydroxybenzoic acids gave 1:1 cocrystals respectively with ornidazole (PABA-ORL and PHBA-ORL) which were found to be isomorphous and isostructural. The isomorphous/isostructural relationship between the two cocrystals was exploited to make their solid solutions, precisely solid solutions of cocrystals (PABA:PHBA-ORL with PABA and PHBA in 0.33:0.67 & 0.46:0.54 ratios in the two structures respectively). Crystal structures of the above adducts are discussed later. Benzoic acid, para-methyl and -iodobenzoic acids respectively formed eutectics with the drug as analyzed in terms of phase diagrams (discussed later). PXRD patterns of cocrystal and eutectic systems are shown in Figures 2 & 3 respectively.

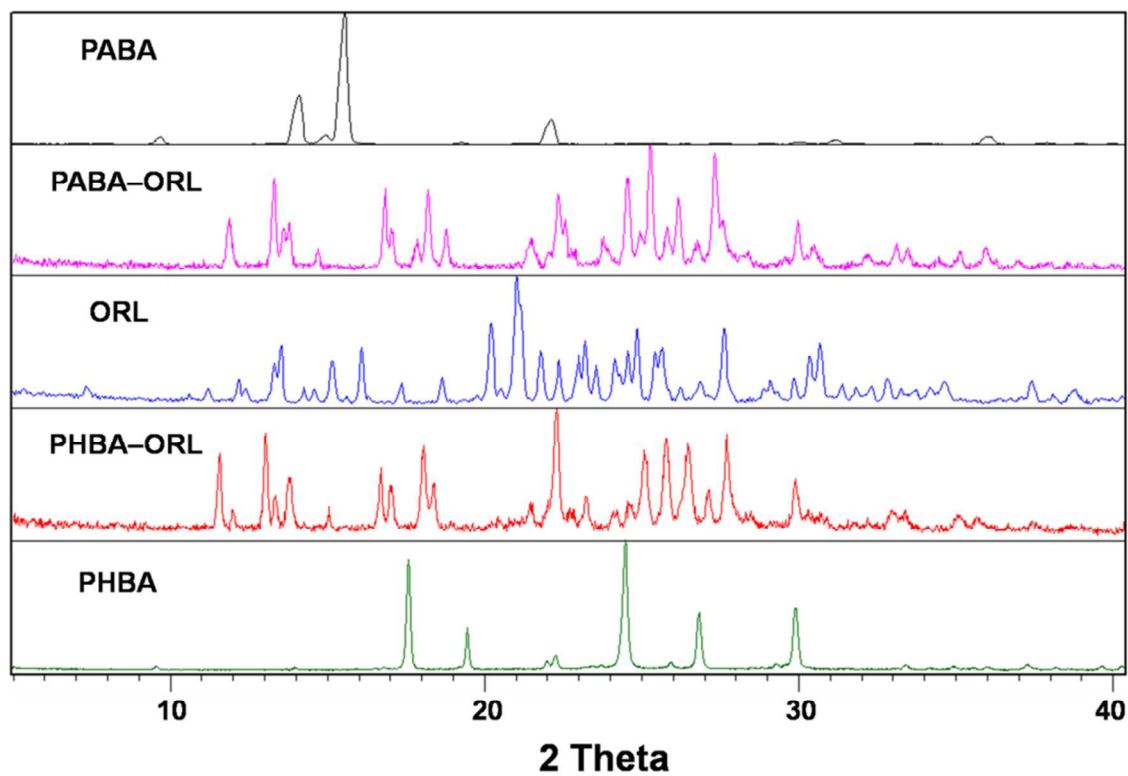
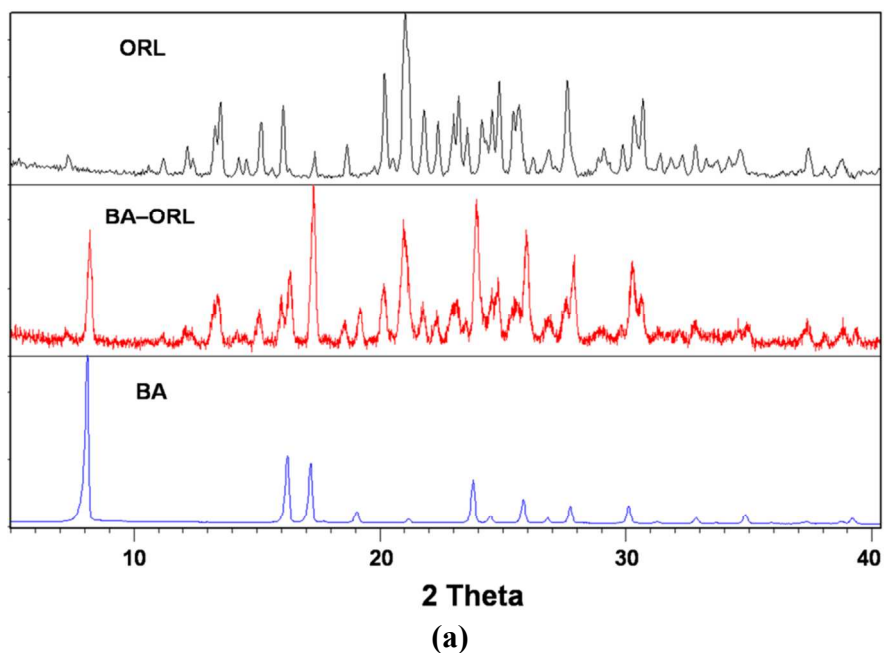
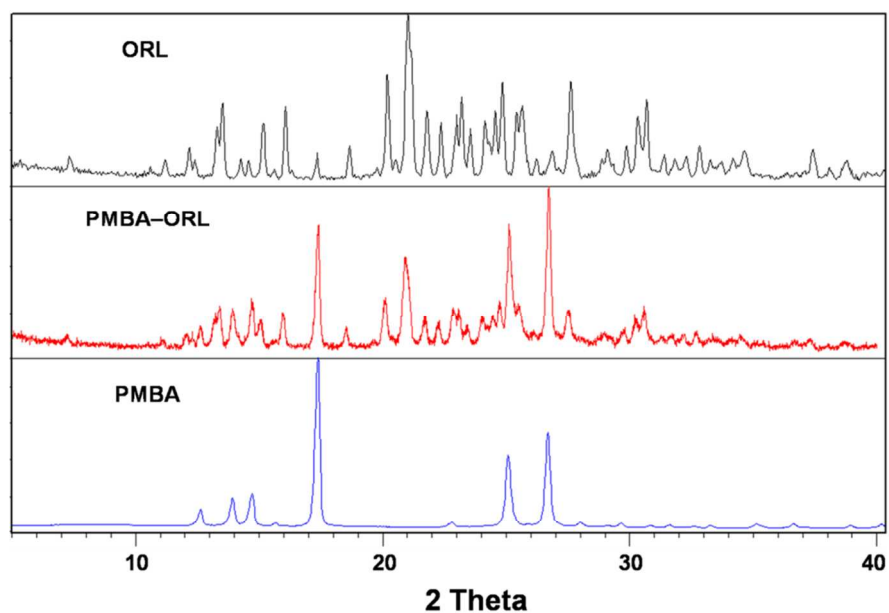
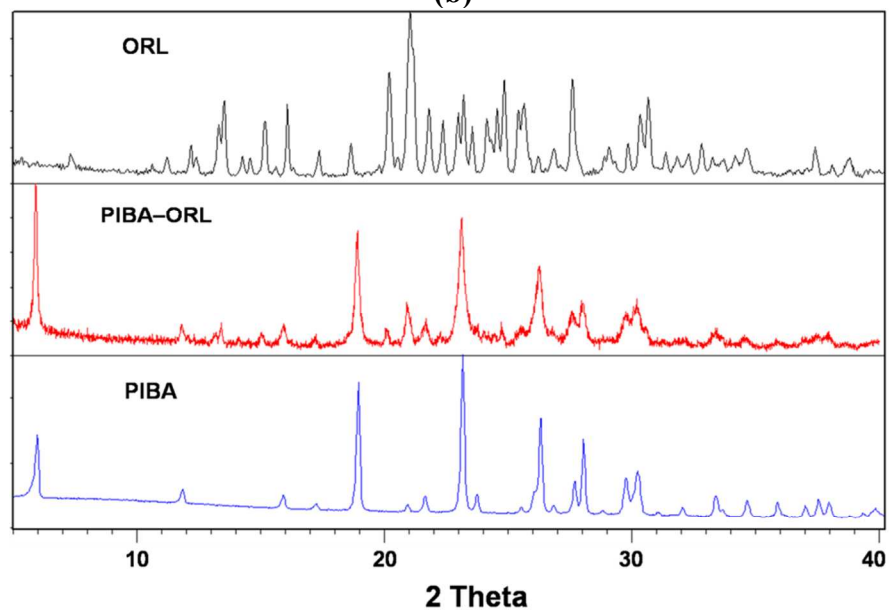


Figure 2 PXR D patterns of PABA-ORL and PHBA-ORL cocrystals are distinct from that of their parent compounds and are identical to each other indicating isostructurality between them.





(b)

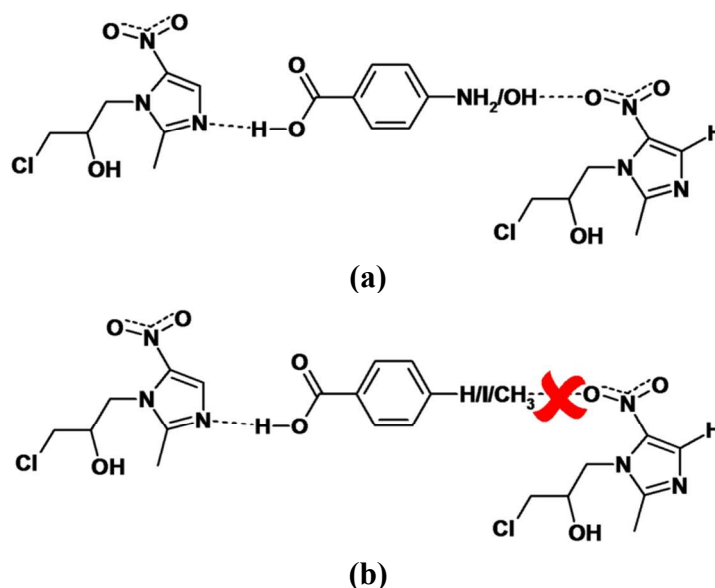


(c)

Figure 3 PXR D patterns of (a) BA-ORL, (b) PMBA-ORL and (c) PIBA-ORL combinations show no new or distinct peaks compared to parent compounds suggesting them to be either simple mixtures or eutectic mixtures. Thermal analysis established the combinations as eutectic systems.

The formation of cocrystal/eutectic for the systems is analyzed as follows. It was established for a binary system with strong hydrogen bonding groups that the primary supramolecular growth unit should be at least three molecules long for a cocrystal to form, and, if the unit is restricted to a finite heterodimer, the combination makes a eutectic.^{2b} The strong hydrogen bonding groups in ornidazole are imidazole and nitro groups which are well-known to form imidazole-carboxylic acid¹⁹ and nitro-amine^{1e}/hydroxyl²⁰/iodo^{3b,21} heterosynthons and can,

therefore, give rise to cocrystals. On this background, benzoic acid and its structural analogues containing the aforementioned complementary functional groups were chosen (Figure 1) by keeping the carboxylic acid group common for all cofomers and varying the functionality at the para position (hydrogen, amine, hydroxyl, methyl and iodo groups) of benzoic acid. Thus, all cofomers can form carboxylic acid–imidazole heterodimeric unit when combined with ornidazole, but, depending on the induction strength complementarity between cofomer's para-functionality and ornidazole's nitro group, the combination can propagate as a cocrystal growth unit or remain as a eutectic dimeric unit. We devised a scheme to show the formation of cocrystal or eutectic for a given combination (Scheme 1) based on the gradation in inductive force strengths of cofomer's para-functionality (decreasing $+I$ effect: $\text{NH}_2 > \text{OH} > \text{I} > \text{CH}_3 > \text{CH}$) with respect to ornidazole's highly $-I$ nitro group.



Scheme 1 (a) PABA and PHBA form cocrystals with ORL as the propagation of carboxylic acid–imidazole heterodimer takes place by strongly complementary amine/hydroxyl–nitro interactions. (b) BA, PIBA and PHBA lacking viable inductive donor groups to complement the strong nitro acceptor cannot make supramolecular growth units beyond finite acid–imidazole heterodimers with ORL and therefore give rise to eutectics.

PABA and PHBA by forming strong amine/hydroxyl–nitro interactions respectively, in accordance to induction strength complementarity (high $+I$ vs. high $-I$ effect) between the groups, make supramolecular units beyond acid–imidazole heterodimer with ORL (Scheme 1) and therefore resulted in cocrystals. BA, PMBA and PIBA respectively gave eutectics with the drug due to mismatch between their weakly inductive donor groups ($-\text{CH}$, $-\text{CH}_3$ and $-\text{I}$) and the strong nitro acceptor (low $+I$ vs. high $-I$ effect) for viable heteromolecular interactions (as compared to PABA/PHBA) (Scheme 1). As a result, the combinations cannot propagate as a cocrystal growth unit, but the plausibility of discrete imidazole–acid interactions in the lattice space renders them to be eutectic systems. PIBA–ORL combination is a border-line case, wherein the facile iodo–nitro heterosynthon could have given rise to a cocrystal, but it manifested as a eutectic system which shows that induction strength and electrostatics have a major role in governing the formation of a cocrystal/eutectic.

X-ray crystal structures of cocrystals (PABA–ORL and PHBA–ORL) and their solid solutions (PABA:PHBA–ORL): The 1:1 PABA–ORL and PHBA–ORL cocrystals are solved in a monoclinic system, space group $P2_1/n$, with similar unit cell dimensions suggesting them to be isomorphous and isostructural.⁴ Crystallographic parameters are given in Table 1. The crystal structures are corrugated sheets formed by anti-parallel tapes of alternate PABA/PHBA and ORL molecules connected by acid–imidazole and amine/hydroxyl–nitro interactions (Figure 4). Based on the isomorphous/isostructural features between the two cocrystals, solid solutions between them were attempted and two were successfully isolated. Understandably, both the solid solutions are isomorphous and isostructural to their parent cocrystals (Table 1 & Figure 4). The integrity of the solid solution is established by low *R*-factor achieved upon assigning both nitrogen (of PABA amine component) and oxygen (of PHBA hydroxyl component) at the same position in the refinement model. Consequent occupancy refinements resulted in 0.33:0.67 and 0.46:0.54 ratios of PABA:PHBA in the two solid solutions. The assignment of these occupancies is analyzed by difference Fourier maps (Figure 5) generated with full occupancy of individual components and compared with that of amine+hydroxyl refinement model. The residual density at individual nitrogen atom or oxygen atom (Figure 5) validates the occupancy assignment of amine+hydroxyl refinement model. On the other hand, not surprisingly, the thermal behavior of solid solutions is different from their parent cocrystals and is discussed next.

Table 1 Crystallographic parameters.

Compound	PABA–ORL	PHBA–ORL	PABA(0.46):PHBA(0.54)–ORL	PABA(0.33):PHBA(0.67)–ORL
Formula	C ₁₄ H ₁₇ N ₄ O ₅ Cl	C ₁₄ H ₁₆ N ₃ O ₆ Cl	C ₁₄ H _{16.5} ClN _{3.5} O _{5.5}	C ₁₄ H _{16.25} ClN _{3.25} O _{5.75}
Formula weight	356.8	357.8	357.3	357.5
Crystal system	monoclinic	monoclinic	monoclinic	monoclinic
Space group	$P2_1/n$	$P2_1/n$	$P2_1/n$	$P2_1/n$
a (Å)	7.136(4)	6.976(3)	7.028(5)	7.062(9)
b (Å)	14.890(9)	15.246(8)	15.083(1)	15.067(1)
c (Å)	14.839(7)	14.610(7)	14.752(1)	14.783(1)
β (°)	91.63(5)	91.60(4)	90.09(6)	90.56(9)
Volume (Å ³)	1576.1(1)	1553.3(2)	1564.0(2)	1573.1(3)
Z*	8	8	8	8
T (K)	120	120	120	120
Density (g cm ⁻³)	1.50	1.53	1.52	1.51
μ (mm ⁻¹)	0.277	0.284	0.280	0.280
F (000)	743.9	743.9	743.9	743.9
No. of measured reflections	13240	12961	7417	7606
No. of unique reflections	3098	3056	2957	2931
No. of	2386	2029	2261	2278

reflections used				
$R_{\text{all}}, R_{\text{obs}}$	0.069, 0.048	0.097, 0.062	0.082, 0.062	0.074, 0.055
$wR_{2_{\text{all}}}, wR_{2_{\text{obs}}}$	0.109, 0.097	0.176, 0.148	0.165, 0.152	0.146, 0.135
$\Delta\rho_{\text{min,max}}$ ($e \text{ \AA}^{-3}$)	-0.262, 0.654	-0.364, 0.510	-0.561, 0.625	-0.580, 0.588
GOOF	1.038	1.041	1.053	1.034
CCDC No.	1020267	1020268	1014220	1020269

* $Z = Z''$ (no. of crystallographically non-equivalent molecules of any type in the asymmetric unit)²² \times no. of independent general positions of the space group.

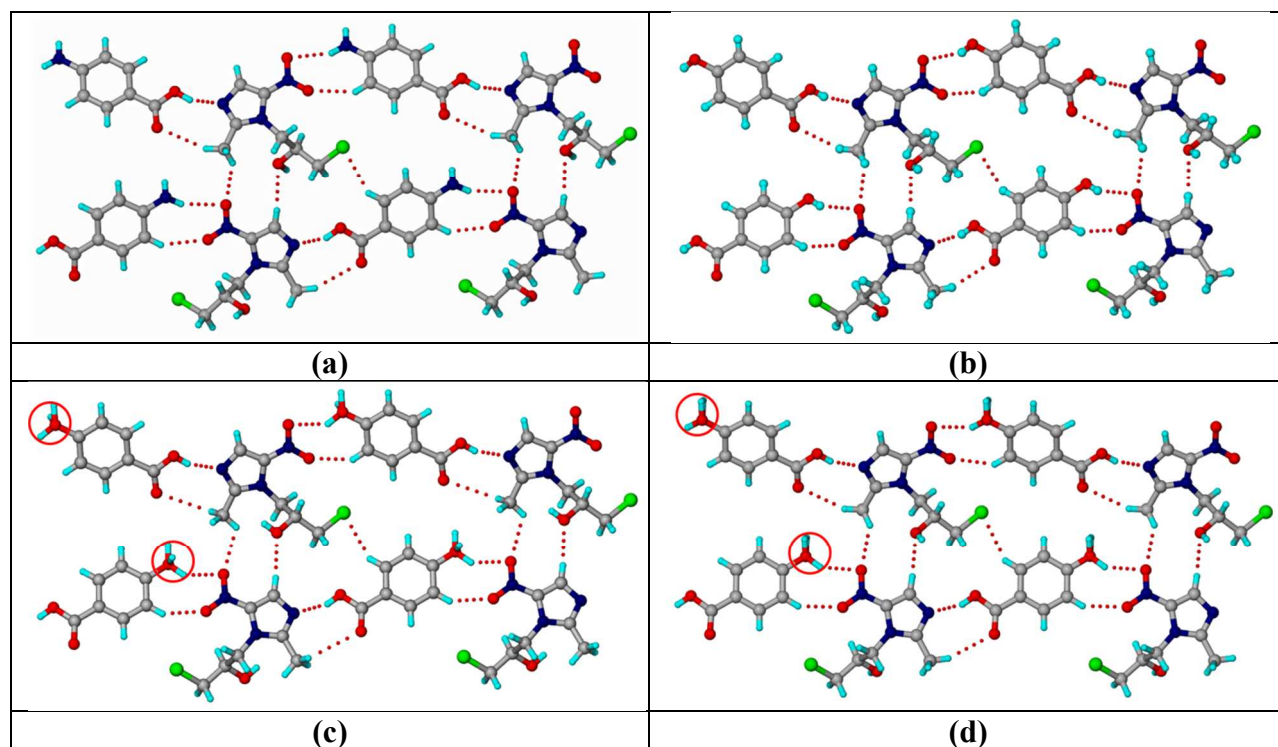


Figure 4 (a) PABA–ORL and (b) PHBA–ORL isostructural cocrystals. Anti-parallel tapes of alternate PABA/PHBA and ORL molecules connected by acid–imidazole and amine/hydroxyl–nitro interactions extend into corrugated sheets through C–H \cdots O and C–H \cdots Cl bonds. (c) PABA(0.46):PHBA(0.54)–ORL and (d) PABA(0.33):PHBA(0.67)–ORL solid solutions are isostructural to their parent cocrystals. Amine/hydroxyl position is indicated in red circle.

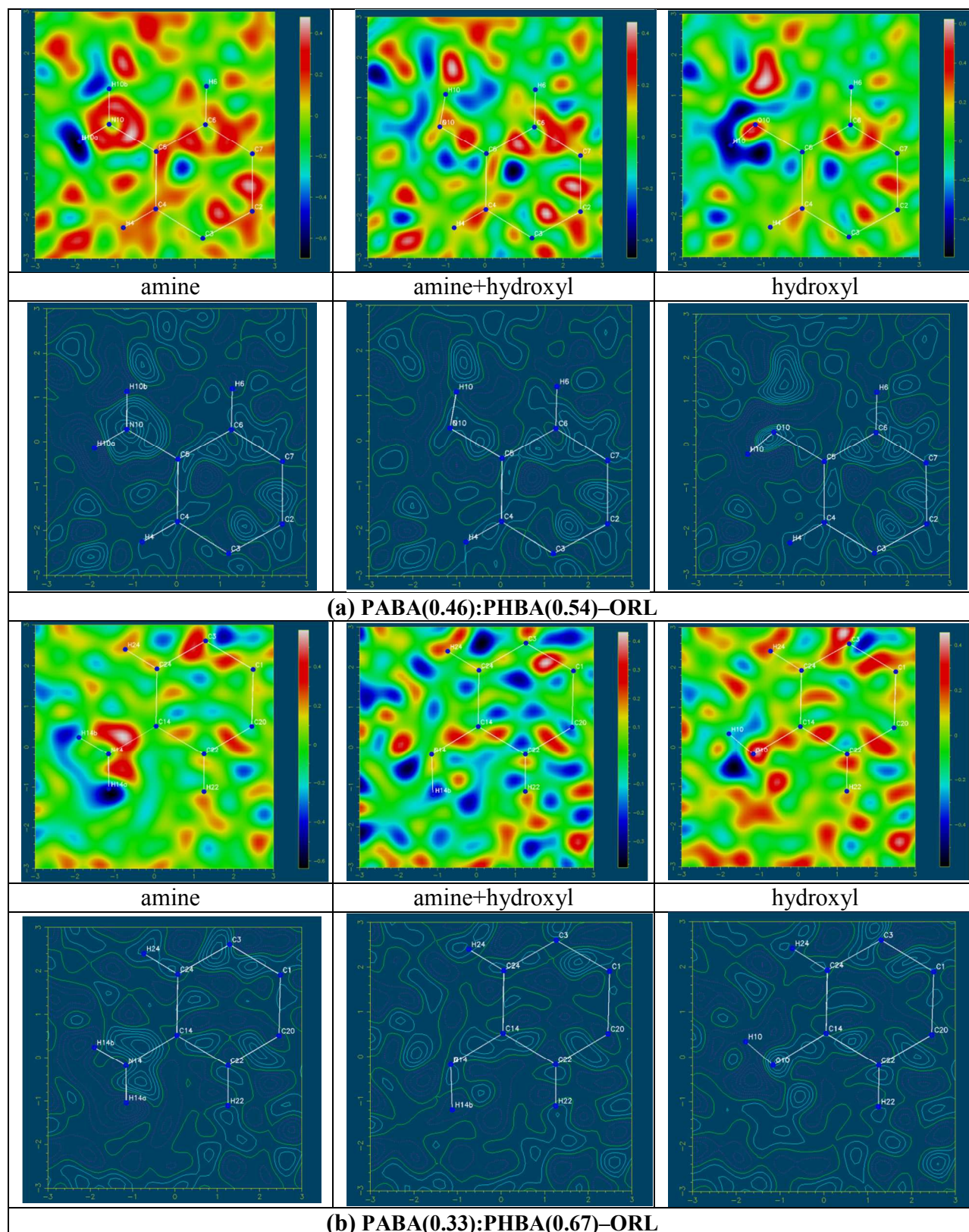


Figure 5 Difference Fourier maps and contour plots of (a) PABA(0.46):PHBA(0.54)–ORL and (b) PABA(0.33):PHBA(0.67)–ORL solid solutions show lower residual density on amine+hydroxyl model upon refinements.

Thermal analysis: DSC on PABA–ORL and PHBA–ORL cocrystals established them to exhibit intermediate melting points compared to their parent compounds (Figure 6). Similarly, PABA:PHBA–ORL solid solutions exhibited intermediate melting points compared to their parent cocrystals (Figure 6). The melting points of the cocrystals and also their solid solutions are found to be proportional to that of their parent materials (Table 2). High melting PHBA (215 °C) resulted in higher melting cocrystal (PHBA–ORL 134 °C) and solid solutions (127 & 123 °C; both contain higher amount of PHBA) and low melting PABA (187 °C) gave lower melting cocrystal (PABA–ORL 118 °C).

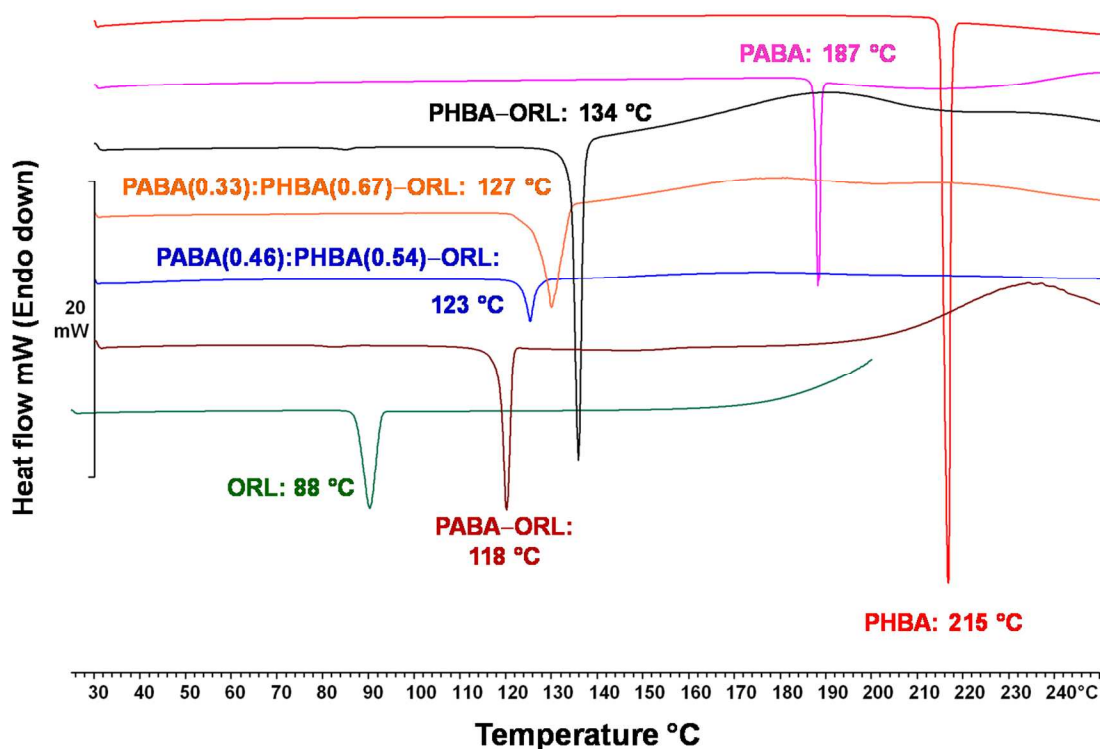


Figure 6 DSC of cocrystals and their solid solutions compared with their parent materials.

Table 2 Melting points of the compounds in °C.

ORL: 88		
Cofomer	Adduct	
PABA: 187	PABA–ORL: 118	PABA(0.46):PHBA(0.54)–ORL: 123
PHBA: 215	PHBA–ORL: 134	PABA(0.33):PHBA(0.67)–ORL: 127
BA: 122	BA–ORL: 58	
PMBA: 178	PMBA–ORL: 78	
PIBA: 227 (melt cum decomposition)	PIBA–ORL: 84	

Phase diagram analysis is known to simultaneously establish a given combination as a eutectic system and rule out the possibility of cocrystal formation (also in a different stoichiometric ratio).^{2b,23} Hence, we constructed phase diagrams for BA/PMBA/PIBA-ORL combinations. At first, we examined the eutectic behavior of the three combinations in 1:1 ratio by DSC (Figure 7). Later, different molar compositions (1:2, 2:1, 1:3, 3:1, 1:4 & 4:1) for each of the combinations were analyzed on a melting point apparatus and the solidus/liquidus events were plotted. Only a single invariant low melting point is observed in common for all the different compositions of each combination and all the three combinations exhibited 'V'-type phase diagram characteristic of a eutectic system (Figure 8). Based on the solidus-liquidus behavior monitored on the melting point apparatus, the eutectic composition of each system is estimated to be 1:2 for BA-ORL and 1:4 for PMBA-ORL and PIBA-ORL respectively (Figure 8). Similar to the correlation observed between the melting points of cocrystals/solid solutions with their parent materials, the melting points of the eutectics are proportional to their parent materials (Table 2).

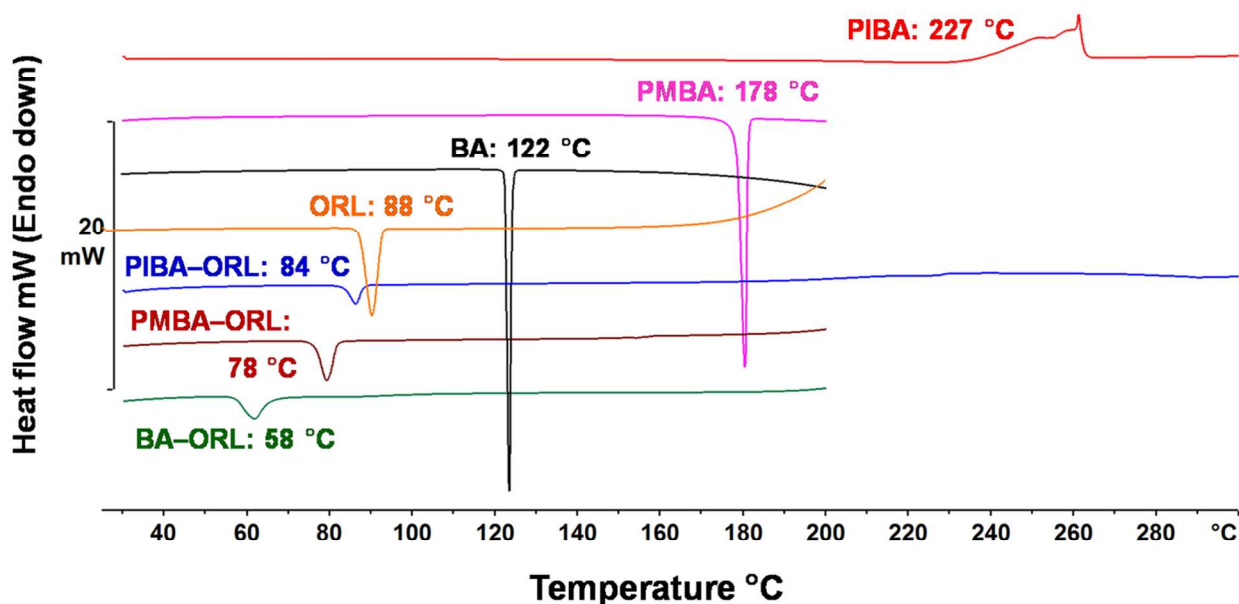
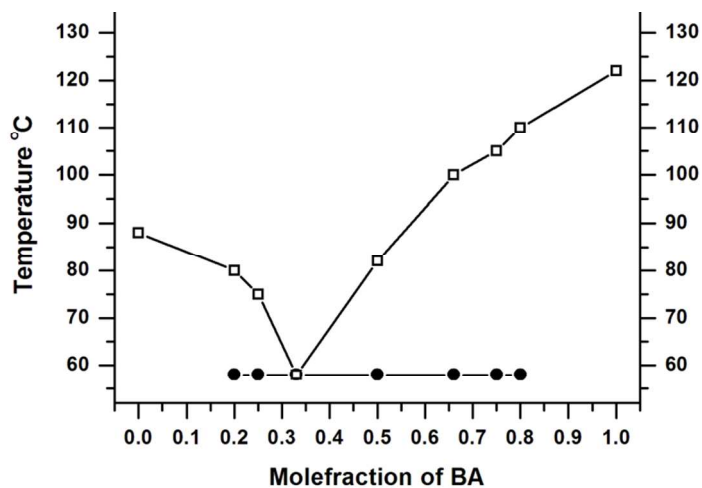
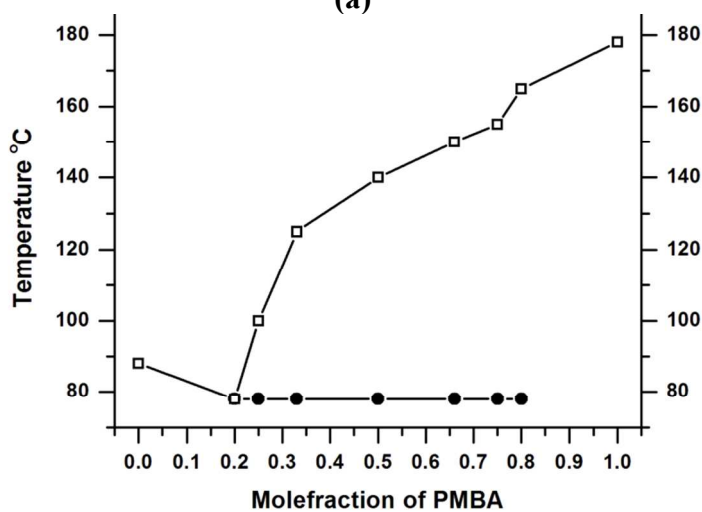


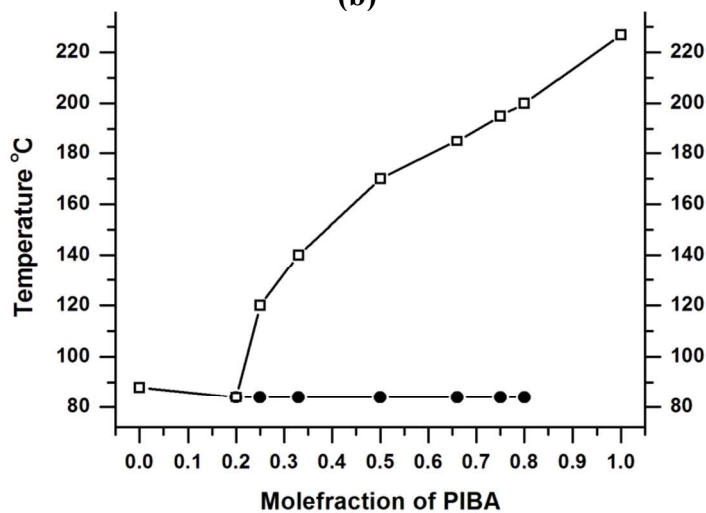
Figure 7 DSC of 1:1 BA-ORL, PMBA-ORL and PIBA-ORL combinations exhibit eutectic-type behavior.



(a)



(b)



(c)

Figure 8 Binary phase diagrams of (a) BA-ORL, (b) PMBA-ORL and (c) PIBA-ORL eutectic systems. Solidus points are shown as filled circles and liquidus points as open squares. The eutectic composition is 1:2 for (a) and 1:4 for (b) and (c) respectively.

Conclusions

We show that the inductive effect affects the outcome of cocrystallization experiment based on which one can tune the formation of cocrystals and eutectics. We performed cocrystallization of ornidazole with the intent of steering its supramolecular solid form space and obtain desired cocrystallization products. New cocrystals and eutectics of the drug were obtained complying with our design strategy. A less explored case of cocrystals forming solid solutions was also reported. Melting point correlations between adducts and their parent compounds are consistent with the trends observed in the graded organic systems.^{1b,2a,b,6} In this study, we found that the relative differences in inductive force strengths of cofomers can tend to vary the interaction strengths between complementary hydrogen bonding groups, in effect, leading to formation of different adducts (cocrystals or eutectics). Thus, an improved understanding on the phenomenon of cocrystallization in terms of molecular recognition and binding which is significant from both fundamental and application facets has been attained.

Experimental Section

Materials

Commercially available ornidazole (Sigma-Aldrich, Bengaluru, India) and all other compounds (Alfa Aesar, Bengaluru, India) were used without further purification. Solvents were of analytical or chromatographic grade and purchased from local suppliers.

Methods

Solid state grinding

Compounds in molar ratios combined together in a 100 mg scale were subjected to manual grinding for 15 min using a mortar-pestle. The ground materials were analyzed by powder X-ray diffraction (PXRD) and thermal techniques to ascertain the formation of cocrystal or eutectic.

Evaporative crystallization

1:1 PABA–ORL cocrystal: Ground mixture of PABA (14 mg, 0.1 mmol) and ornidazole (22 mg, 0.1 mmol) was dissolved in 5 mL methanol and left for slow evaporation at room temperature. Light yellow block crystals were obtained after a few days upon solvent evaporation.

1:1 PHBA–ORL cocrystal: Ground mixture of PHBA (14 mg, 0.1 mmol) and ornidazole (22 mg, 0.1 mmol) was dissolved in 5 mL methanol and left for slow evaporation at room temperature. Light yellow block crystals were obtained after a few days upon solvent evaporation.

PABA:PHBA–ORL solid solutions: PABA and PHBA taken together (in 4 & 10 mg (0.025 & 0.075 mmol) and vice-versa respectively in two batches) were mixed with ornidazole (22 mg, 0.1 mmol) and dissolved in 5 mL methanol. Light red block crystals were obtained after a few days upon solvent evaporation at room temperature.

X-ray crystallography

X-ray reflections for PABA–ORL, PHBA–ORL and PABA:PHBA–ORL were collected at 120 K on an Oxford Xcalibur Mova E diffractometer equipped with an EOS CCD detector and a microfocus sealed tube using Mo K α radiation ($\lambda = 0.7107 \text{ \AA}$). Data collection and reduction was performed using CrysAlisPro (version 1.171.36.32)²⁴ and OLEX2 (version 1.2)²⁵ was used to solve and refine the crystal structures. All non-hydrogen atoms were refined anisotropically. In

case of solid solutions, all hydrogen atoms were fixed by considering the riding hydrogen atom model. Hydrogen atoms on heteroatoms were located from difference Fourier maps in case of cocrystals. All C–H atoms were fixed geometrically. The final CIF files were validated in PLATON.²⁶

Powder X-ray Diffraction

PXRD were recorded on PANalytical X'Pert diffractometer using Cu-K α X-radiation ($\lambda = 1.54056 \text{ \AA}$) at 40 kV and 30 mA. X'Pert HighScore Plus (version 1.0d)²⁷ was used to collect and plot the diffraction patterns. Diffraction patterns were collected over 2θ range of 5–40° using a step size of 0.06° 2θ and time per step of 1 sec.

Thermal analysis

DSC was performed on a Mettler Toledo DSC 822e module with samples placed in crimped but vented aluminum pans. Samples of 1–3 mg were heated @ 5 °C min⁻¹ in the temperature range 30–300 °C and were purged by a stream of dry nitrogen flowing at 50 mL min⁻¹. Different compositions of eutectic-forming combinations were analyzed for their solidus-liquidus temperatures on a Labindia visual melting range apparatus (MR 13300710) equipped with a camera and a LCD monitor.

Packing Diagrams

X-Seed²⁸ was used to prepare packing diagrams.

Acknowledgements

KDP thanks the CSIR for Senior Research Fellowship and SC thanks the UGC for Dr. D. S. Kothari Postdoctoral Fellowship. LDS thanks the IAS for Summer Research Fellowship Program. TNG thanks the DST for J. C. Bose Fellowship. We thank Dr. Diptikanta Swain for his help in solving X-ray crystal structures of solid solutions.

References

- (a) N. Shan and M. J. Zaworotko, *Drug Discov. Today*, 2008, **13**, 440–446; (b) N. Schultheiss and A. Newman, *Cryst. Growth Des.*, 2009, **9**, 2950–2967; (c) D. Braga, F. Grepioni, L. Maini, S. Prosperi, R. Gobetto and M. R. Chierotti, *Chem. Commun.*, 2010, **46**, 7715–7717; (d) D. Yan, A. Delori, G. O. Lloyd, T. Frišćić, G. M. Day, W. Jones, J. Lu, M. Wei, D. G. Evans and X. Duan, *Angew. Chem. Int. Ed.*, 2011, **50**, 12483–12486; (e) S. Cherukuvada, N. J. Babu and A. Nangia, *J. Pharm. Sci.*, 2011, **100**, 3233–3244; (f) C. B. Aakeröy, S. Forbes and J. Desper, *CrystEngComm*, 2014, **16**, 5870–5877; (g) R. Kaur, S. S. R. Perumal, A. J. Bhattacharya, S. Yashonath and T. N. G. Row, *Cryst. Growth Des.*, 2014, **14**, 423–426; (h) G. R. Desiraju, *Angew. Chem. Int. Ed.*, 1995, **34**, 2311–2327.
- (a) S. Cherukuvada and A. Nangia, *Chem. Commun.*, 2014, **50**, 906–923; (b) S. Cherukuvada and T. N. G. Row, *Cryst. Growth Des.*, 2014, **14**, 4187–4198; (c) A. Delori, P. Maclure, R. M. Bhardwaj, A. Johnston, A. J. Florence, O. B. Sutcliffe and I. D. H. Oswald, *CrystEngComm*, 2014, **16**, 5827–5831.
- (a) P. A. Wood, N. Feeder, M. Furlow, P. T. A. Galek, C. R. Groom and E. Pidcock, *CrystEngComm*, 2014, **16**, 5839–5848; (b) S. Tothadi and G. R. Desiraju, *Chem. Commun.*, 2013, **49**, 7791–7793; (c) A. Bialonska and Z. Ciunik, *CrystEngComm*, 2013, **15**, 5681–5687; (d) C. C. Seaton, K. Chadwick, G. Sadiq, K. Guo and R. J. Davey, *Cryst. Growth Des.*, 2010, **10**, 726–733; (e) C. B. Aakeröy, J. Desper, M. E. Fasulo, I. Hussain, B. Levin and N. Schultheiss, *CrystEngComm*, 2008, **10**, 1816–1821.
- (a) http://reference.iucr.org/dictionary/Isomorphous_crystals; (b) http://reference.iucr.org/dictionary/Isostructural_crystals; (c) A. Kalman, L. Parkanyi and G. Argay, *Acta Crystallogr. Sect. B: Struct. Sci.*, 1993, **49**, 1039–1049; (d) N. K. Nath, B. K. Saha and A. Nangia, *New J.*

- Chem.*, 2008, **32**, 1693–1701; (e) Md. A. Masood and G. R. Desiraju, *Chem. Phys. Lett.*, 1986, **130**, 199–202.
5. (a) M. A. Oliveira, M. L. Peterson and D. Klein, *Cryst. Growth Des.*, 2008, **8**, 4487–4493; (b) M. Dabros, P. L. Emery and V. R. Thalladi, *Angew. Chem. Int. Ed.*, 2007, **46**, 4132–4135.
6. J. Clayden, N. Greeves, S. Warren and P. Wothers, *Organic Chemistry*, Oxford University Press, 2001.
7. (a) E. Arunan, G. R. Desiraju, R. A. Klein, J. Sadlej, S. Scheiner, I. Alkorta, D. C. Clary, R. H. Crabtree, J. J. Dannenberg, P. Hobza, H. G. Kjaergaard, A. C. Legon, B. Mennucci and D. J. Nesbitt, *Pure Appl. Chem.*, 2011, **83**, 1637–1641; (b) G. R. Desiraju, P. S. Ho, L. Kloo, A. C. Legon, R. Marquardt, P. Metrangolo, P. Politzer, G. Resnati and K. Rissanen, *Pure Appl. Chem.*, 2013, **85**, 1711–1713.
8. (a) M. Bakshi, B. Singh, A. Singh and S. Singh, *J. Pharm. Biomed. Anal.*, 2001, **26**, 891–897; (b) <http://www.panaceabiotec.com/product-pdf/Giro.pdf>.
9. Indian Pharmacopoeia, 2010, **3**, 1808–23.
10. <http://www.panaceabiotec.com/product-pdf/Ocimix.pdf>.
11. P. Rutgeerts, G. V. Assche, S. Vermeire, G. D'Haens, F. Baert, M. Noman, I. Aerden, G. D. Hertogh, K. Geboes, M. Hiele, A. D'Hoore and F. Penninck, *Gastroenterology*, 2005, **128**, 856–861.
12. (a) J. Hu and L. R. McDougald, *Vet. Parasit.*, 2004, **121**, 233–238; (b) Y. Marcus and M. Gurevitz, *WO Pat.*, 2014/006617 A1, 2014.
13. (a) Y. Wang, C. Zhang and X. Tao, *US Pat.*, 2013/0202698 A1, 2013; (b) C. Yang, J. Qiang and X. Liu, *CN Pat.*, 102516299 A, 2012.
14. K. M. Anderson, M. R. Probert, C. N. Whiteley, A. M. Rowland, A. E. Goeta and J. W. Steed, *Cryst. Growth Des.*, 2009, **9**, 1082–1087.
15. L. Deng, W. Wang and J. Lv, *Acta Crystallogr. Sect. E: Struct. Rep. Online*, 2007, **63**, o4204.
16. R. K. Maheswari, V. V. Srivastav, R. R. Prajapat, A. Jain, P. Kamaria and S. Sahu, *Indian J. Pharm. Sci.*, 2010, **72**, 258–261.
17. F. I. Khattab, N. K. Ramadan, M. A. Hegazy and N. S. Ghoniem, *Pharmaceut. Anal. Acta*, 2012, **3**, 1000179.
18. A. V. Trask and W. Jones, *Top. Curr. Chem.*, 2005, **254**, 41–70.
19. (a) D. -K. Bucar, R. F. Henry, X. Lou, R. W. Duerst, T. B. Borchardt, L. R. MacGillivray and G. G. Zhang, *Mol. Pharm.*, 2007, **4**, 339–346; (b) L. Wang, L. Zhao, M. Liu, R. Chen, Y. Yang and Y. Gu, *Sci. China Chem.*, 2012, **55**, 2115–2122.
20. (a) A. Alhalaweh, S. George, S. Basavoju, S. L. Childs, S. A. A. Rizvi and S. P. Velaga, *CrystEngComm*, 2012, **14**, 5078–5088; (b) V. R. Vangala, P. S. Chow and R. B. H. Tan, *CrystEngComm*, 2011, **13**, 759–762.
21. (a) L. S. Reddy, S. K. Chandran, S. George, N. J. Babu and A. Nangia, *Cryst. Growth Des.*, 2007, **7**, 2675–2690; (b) R. Thaimattam, C. V. K. Sharma, A. Clearfield and G. R. Desiraju, *Cryst. Growth Des.*, 2001, **1**, 103–106.
22. B. P. van Eijck and J. Kroon, *Acta Crystallogr. Sect. B: Struct. Sci.*, 2000, **56**, 535–542.
23. (a) S. -W. Zhang, M. T. Harasimowicz, M. M. de Villiers and L. Yu, *J. Am. Chem. Soc.*, 2013, **135**, 18981–18989; (b) R. E. Davis, K. A. Lorimer, M. A. Wilkowski, J. H. Rivers, K. A. Wheeler and J. Bowers, *ACA Trans.*, 2004, **39**, 41–61.
24. CrysAlisPro, ver. 1.171.36.32, Agilent Technologies UK Ltd: Yarnton, England, 2011.
25. O. V. Dolomanov, A. J. Blake, N. R. Champness and M. Schröder, *J. Appl. Crystallogr.*, 2003, **36**, 1283–1284.
26. A. L. Spek, *PLATON: A Multipurpose Crystallographic Tool*, Utrecht University, Utrecht, The Netherlands, 2002.
27. X'Pert HighScore Plus, *The complete powder analysis tool*, PANalytical B. V. 2003.
28. L. J. Barbour, *X-Seed, Graphical Interface to SHELX-97 and POV-Ray, Program for Better Quality of Crystallographic Figures*; University of Missouri-Columbia, Columbus, MO, 1999.